Synthesis and Evaluation of a Surface-Active Photoinitiator for Microemulsion Polymerization

Lijuan Wang, Xuejun Liu, and Yuzhuo Li*

Department of Chemistry, Clarkson University, Potsdam, New York 13699-5810

Received June 23, 1997; Revised Manuscript Received March 13, 1998

ABSTRACT: The first water-soluble perester that can serve as a surface-active photoinitiator for polymerization has been synthesized. This photoinitiator showed a good solubility in water and a sufficient molar absorptivity in the UVA region. While heat-activated decomposition of this peroxide in an aqueous solution leads mainly to heterolytic cleavage of the dioxy bond, its photochemical decomposition gives predominately homolytic cleavage. When the perester was used as an initiator in microemulsion polymerization of styrene, stable and relative monodispersed polystyrene latices were obtained. The produced polystyrene has a high molecular weight in the range of 10^4-10^6 and a narrow molecular weight distribution (MWD = $M_w/M_n \sim 2.5$). The initiator is located at the interface, and the polymerization may be initiated with the separation of two radicals which are generated at the interface. The latex characteristics such as particle size, polydispersity, molecular weight, and molecular weight distribution depend on the nature of the surfactant and the way by which the radicals are generated.

Introduction

Photopolymerization that utilizes electromagnetic radiation as the energy source for polymerization of monomers, oligomers, and prepolymers has been found in many important industrial processes with a wide range of applications.[1] The increasing popularity of photopolymerization process has led to the demand for various specialty photoinitiators that possess desirable properties, such as a greater initiation efficiency for a higher polymerization rate and/or lower monomer residue concentration, and a greater compatibility with reaction medium.[2−5] Owing to the increasing interest of nonorganic solvent processes, such as aqueous dispersed coatings, water-soluble photoinitiators have received increasing attention. New water-soluble photoinitiators have been developed by introducing ionic groups (quaternary ammonium salts,[6−8] sulfonate,[6−8] and phosphinate[9]) or a hydrophilic chain[10] into oil-soluble initiators which are known to exhibit high activities in nonaqueous solvents.

Although hydrogen peroxide and some alkyl hydroperoxides and peracids are soluble in water, a clean homolysis of their dioxy bonds is not commonly observed except in some metal-catalyzed decompositions.[11] In addition, the stabilities of alkyl hydroperoxides and peracids are often less than adequate. Peresters and dialkyl peroxides yield radicals readily upon decomposition. They are, however, generally insoluble in water. Recently we have synthesized a number of water-soluble dialkyl peroxides and peresters[12] that can be thermally activated as polymerization initiators. One of the examples is the quaternary ammonium salt of Lupersol 70, perester **1**, as shoown in Chart 1. Yet, there have been no literature reports of any photoactive water-soluble organic peroxides. In this paper, we report the synthesis and evaluation of the first water-soluble perester which can serve as a photoinitiator in the microemulsion polymerization of styrene.

Although the concept of microemulsion was introduced as early as in 1943 by Hoar and Schulman,[13] it is only within the past decade that microemulsions were extensively and systematically studied.[1] Developed in

Chart 1

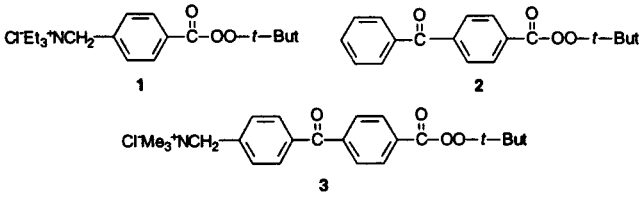

1980s, microemulsion polymerization has attracted a great deal of attention and become an increasingly growing field of research in polymer synthesis.[14−20] Microemulsion polymerization can yield nanosized stable latices that are not easily obtained from other systems.[14] Polymerization kinetics in both types of microemulsions (O/W or W/O) can be described by the Candau−Leong−Fitch model, which suggested that the polymerization is initiated with the entry of radicals to monomer droplets and that particles grow by recruiting monomer droplets.[21−24] The particle size of styrene latices has been shown to have good correlation with the relative amount of surfactant.[25] To eliminate possible chain-transfer reactions or destabilization of the polymer latex caused by alcohol cosurfactant, polymerization in alcohol-free ternary microemulsions have also been investigated.[26−29]

Microemulsions are particularly suitable for photochemical reactions because of their transparent property in the UV−visible region. For example, photoinduced polymerization of styrene in a water/SDS/pentanol/styrene−toluene microemulsion system with dibenzyl ketone (DBK) has been investigated by Turro and El-Aasser.[30] The microemulsion remained transparent during the entire polymerization process. The molecular weights of polymers can be controlled by light intensity and irradiation time. Unlike heat-activated initiators, a photoinitiator decomposes at room temperature. It causes much less disturbance to the phase structure of the microemulsion.

For emulsion or microemulsion polymerization, an initiator could be either located in the water or oil phase. Persulfates have been traditionally used as water-phase

S0024-9297(97)00907-8 CCC: $15.00
Published on Web 05/08/1998

initiators. One of the disadvantages of using persulfates is the generation of hydrosulfuric acid as a byproduct upon decomposition, which may lead to product corrosion. In latex production, it is very much desirable to completely convert monomers into polymers, as residual monomers may give a pungent oder to the end product and/or cause environmental problems. Various means exist to decrease residual monomers in polymers, such as increasing the polymerization temperature, addition of reactive comonomer, and/or selection of proper initiators. It has been found that organic peroxides are much more effective than persulfates as monomer scavengers to reduce the level of unreacted monomers in latex. This is largely due to the hydrophobicity of the radicals generated from organic peroxides.

The delivery of alkoxy radicals to the right location, therefore, may be very important. For this purpose, a surface-active peroxide may offer advantages over the conventional oil-soluble peroxides.

The main objective of the present study is to investigate the utility of a water-soluble surface-active peroxide photoinitiator for microemulsion polymerization. In this paper, the synthesis and characterization of the photoinitiator are first described. A comparison is made between the polymerizations with cationic and anionic surfactants followed by a discussion on the polymerization mechanism to illustrate the particle nucleation and growth. The effects from each microemulsion component on the particle size and molecular weight will also be presented.

Experimental Section

General Data. DTAB (99%) and SDS (98%) were obtained from Aldrich and used without any purification. Styrene purchased from Aldrich was distilled under a reduced pressure to remove the inhibitor[23] and stored at 4 °C until use. HPLC grade water from Fisher Scientific was filtered through 0.25 μm syringe filters and used in all polymerizations. The mass spectra were recorded on a VG ZAB-SE spectrometer. ^{1}H and ^{13}C NMR spectra were obtained on a Bruker AC 250 MHz spectrometer and IR spectra on a 2020 Galaxy Series FT-IR. UV/vis spectra were determined using an HP 8452A Diode Array Spectrophotometer.

Synthesis of 4-(4′-Bromomethylbenzoyl)benzoic Acid Methyl Ester, 5. Compound **5** was prepared by α-bromination of compound **4** according to a similar procedure described in the literature.[31] A white solid was obtained. Yield: 87.4%. Mp: 114.5−116 °C (lit. 115−117 °C). ^{1}H NMR ($CDCl_3$): δ 3.97 (s, 3H), 4.54 (s, 2H), 7.53 (d, 2H), 7.77−7.85 (m, 4H), 8.16 (d, 2H). ^{13}C NMR ($CDCl_3$): δ 32.3, 52.7, 126.9, 129.3, 129.7, 129.9, 130.6, 130.8, 133.5, 136.9, 166.4, 195.4. IR: 1720, 1649 cm^{-1}. The precursor, 4-(4′-methylbenzoyl)benzoic acid methyl ester **4**, was prepared by esterification of 4-(4′-methylbenzoyl)benzoic acid. Yield: 85.9%. Mp: 123−125 °C (lit. 126 °C[31]). ^{1}H NMR ($CDCl_3$): δ 2.45 (s, 3H), 3.97 (s, 3H), 7.30 (d, 2H), 7.72 (d, 2H), 7.82 (d, 2H), 8.15 (d, 2H). ^{13}C NMR ($CDCl_3$): δ 21.9, 52.6, 129.3, 129.6, 129.8, 130.5, 133.1, 134, 141.9, 144.1, 166.5, 195.9. IR: 1722, 1645 cm^{-1}.

Synthesis of [4-(4′-Methoxycarbonylbenzoyl)benzyl]trimethylammonium Bromide, 6. Compound **6** was synthesized by nucleophilic substitution of **5** with trimethylamine. A mixture of 1.8 g of **5** (5.4 mmol) and trimethylamine (2.5 mL, 33% in ethanol, 10 mmol) in 60 mL of THF was stirred at room temperature for 48 h. The white solid was filtered out and washed with anhydrous ethyl ether (3 × 25 mL). After drying, 1.4 g of a white solid was obtained. Yield: 66.0%. ^{1}H NMR (CD_3OD): δ 3.21 (s, 9H), 3.96 (s, 3H), 4.71 (s, 2H), 7.76 (d, 2H), 7.87−7.91 (m, 4H), 8.16 (d, 2H). ^{13}C NMR (CD_3OD): δ 53.2, 53.6, 69.7, 130.8, 131.2, 131.7, 133.8, 134.6, 135.1, 140.4, 142.1, 167.6, 196.8. IR: 1723, 1659 cm^{-1}. High-resolution (FAB) MS *m*/*z* (M − Br): calcd for $C_{19}H_{22}NO_3$, 312.1562; found, 312.1600.

Synthesis of [4-(4′-Carboxybenzoyl)benzyl]trimethylammonium Chloride, 7. Compound **7** was prepared by hydrolysis of ester **6**. To a solution of compound **6** (1.4 g in 10 mL of water) was added 14 mL of hydrochloric acid (36.5−38%). The mixture was brought to reflux for 20 h while stirring. The mixture was concentrated under a reduced pressure to obtain 1.2 g of a yellowish solid. Yield: 98%. ^{1}H NMR (CD_3OD): δ 3.20 (s, 9H), 4.70 (s, 2H), 7.78 (d, 2H), 7.87−7.95 (m, 4H), 8.18 (d, 2H). ^{13}C NMR (CD_3OD): δ 53.6, 69.8, 131.1, 131.7, 133.8, 134.5, 135, 140, 141.5, 168.8, 196.6. IR: 1713, 1657 cm^{-1}. High-resolution (FAB) MS *m*/*z* (M − Cl): calcd for $C_{18}H_{20}NO_3$, 298.1406; found, 298.1440.

Synthesis of [4-(4′-*tert*-Butyldioxycarbonylbenzoyl)benzyl]trimethylammonium Chloride, 3. Compound **7** (1.2 g, 3.6 mmol) was converted to its acid chloride derivative by refluxing overnight with an excess of thionyl chloride (30 mL, 409 mmol). After removal of the excess thionyl chloride in vacuo and a repeated wash with anhydrous ethyl ether, a yellow solid was obtained. The chloride was dissolved in 40 mL of methylene chloride and cooled to 0 °C. A solution of 6 M *tert*-butyl hydroperoxide in decane (2.2 mL) and pyridine (617 mg) was mixed into 10 mL of methylene chloride. The mixture was added to the above acid chloride solution dropwise at 0 °C. The solution was stirred at 0 °C for 1 h, and the temperature gradually rose to room temperature within 1 h. The reaction mixture was neutralized with sodium bicarbonate solution to pH 7−8 and then concentrated under a reduced pressure to yield a yellowish solid. The solid was extracted with methylene chloride (3 × 30 mL). After the solvent was evaporated under a reduced pressure, a yellowish solid (1.2 g) was obtained. Yield: 75.8%. ^{1}H NMR ($CDCl_3$): δ 1.44 (s, 9H), 3.48 (s, 9H), 5.21 (s, 2H), 7.85−7.90 (m, 6H), 8.10 (d, 2H). ^{13}C NMR ($CDCl_3$): δ 26.4, 53.2, 67.8, 84.6, 127.6, 127.7, 129.4, 130.2, 130.7, 133.7, 141.2, 146.2, 163.7, 194.9. IR: 1757, 1665 cm^{-1}. High-resolution (FAB) MS *m*/*z* (M − Cl): calcd for $C_{22}H_{28}NO_4$, 370.2000; found, 370.2019.

Surface Activity Measurement. The surface activity of perester **3** was obtained by the measurement of surface tension of its aqueous solution at room temperature.

Thermal and Photochemical Decomposition Reactions of Compound 3. The thermal decomposition of compound **3** was carried out in a degassed and sealed 5 mm NMR tube in which 10.2 mg of **3** was dissolved in 1 mL of deuterium oxide. The tube was placed in a water bath with temperature control. At predetermined intervals, the reaction mixture was analyzed by ^{1}H NMR to monitor the residual *tert*-butyl group in **3**. At the end of the experiment, the solvent was evaporated under reduced pressure. The product, in nearly 100% yield, was identified as acid **7** according to its ^{1}H NMR and IR spectra.

For photochemical decomposition, a solution of **3** (5.2 mg or 11.0 mg) in 1 mL of deuterium oxide was prepared. The solution was placed in a 5 mm Pyrex NMR tube, degassed, and sealed. The tube was then placed in front of 350 nm UV lamps and analyzed by ^{1}H NMR at predetermined intervals to monitor the intensity change of the *tert*-butyl group. Accompanied with each run, an NMR tube containing a solution of benzophenone (0.1 M) and benzhydrol (0.1 M) in benzene was also irradiated as an actinometric measurement to determine the photon flux.

Reaction between 3 and Potassium Iodide. An aqueous solution of **3** (3.9 mg in 10 mL of water) was prepared. Potassium iodide (8.1 mg) was added, and the reaction was monitored by UV/vis spectrometer at 352 nm. The same experiment was performed in the presence of SDS (29.1 mg) or DTAB (61.7 mg). The relative initial oxidation rates under these conditions were obtained.

Polymerization. Polymerizations were carried out in 20 mL vials sealed with rubber septa. A solution of surfactant in water was prepared and stirred at room temperature for 2 days to establish equilibrium and then filtered with a 0.25 μm syringe filter. This surfactant solution was then mixed with an aqueous solution of **3**. The monomer, styrene, was then added. For polymerization, the microemulsion system was purged carefully with nitrogen for 10 min and then kept in a

water bath while stirring at 70 °C or in a Rayanet photochemical reactor equipped with 16 8-W UV light bulbs (GE, F8T5-BLB) which emit radiations centered at 350 nm.

Particle Characterization. Polymer latex morphology and particle size were examined with a JEOL JEM-1200 EX transmission electron microscope (TEM) operating at 100 kV. The samples were prepared according to a similar procedure described in the literature.[24] The average diameters of the latex particles were measured with a dynamic light scattering (DLS) system equipped with a BI9000 AT correlator (Brookhaven) in 75 × 12 mm test tubes (Fisher Scientific) covered with Parafilm. An Ion Laser (Model 85, LEXEL Inc.) was used to provide the light source at 514.3 nm. Latices were diluted up to 1000 times with filtered HPLC water before measurements to terminate the polymerization and minimize particle−particle interactions. The measurements were made at 25 ± 0.1 °C with scattering angles at 90°. The size profile of the particles was obtained with CUMULANT analysis.[32,33]

Molecular Weight and Molecular Weight Distribution. The microemulsion latex was poured into a large quantity of ethanol immediately after the polymerization. The precipitated polymers were washed with distilled water and ethanol after filtration and dried under vacuum. The percent conversion was determined gravimetrically. The molecular weight (MW) and molecular weight distribution (MWD = M_w/M_n) were determined by gel permeation chromatography (GPC) using a Hewlett-Packard 1050 HPLC equipped with a Phenogel 5 Linear (2) column (300 × 7.8 mm, Phenomenex) and a UV detector at 254 nm. Tetrahydrofuran (THF) was used as eluent (1.0 mL/min at 35 °C) for GPC. Polystyrene standards (2.5 mg/mL in THF, MW 10^5−10^6) purchased from Phenomenex were used for the MW and MWD calibration curves.

Results and Discussion

Synthetic Design. Irradiation of organic peroxides carrying a chromophore initially gives the excited state of the molecule, which then undergoes an intramolecular energy transfer to the dioxy bond and often results in a homolytic cleavage of the dioxy group.[34] A practical photoinitiator should have a sufficiently high molar absorptivity in the desired wavelength region and a high quantum yield for radical production.[35] Benzoyl peroxide, *tert*-butyl perbenzoate, and dialkyl peroxides are widely used as thermal initiators for free radical chain reactions. Their potential as photoinitiators is low due to their relatively weak absorptions in the UVA (>320 nm) region where most monomers absorb less strongly. To enhance light absorption efficiency at longer wavelengths, perester derivatives of well-known triplet sensitizers such as benzophenone[2,36,37] and fluorenone[38,39] have been prepared. One of the examples is the *tert*-butyl perester derivative of benzophenone,[2] shown as compound **2** in Chart 1. Its n → π^* transition extends the absorption >300 nm and leads to a triplet excited state with long lifetime. The triple excited state usually has sufficient energy (approximately twice that of the dioxy bond dissociation energy in a perester) and are well suited for the decomposition of a dioxy functional group via intramolecular energy transfer. In this study, we incorporated both a quarternary ammonium functional group (as in compound **1**) to enhance water solubility and a benzophone moiety (as in compound **2**) to extend the UV absorption wavelengths into a new photoinitiator, perester **3**.

Synthesis and Characterization. The synthesis of **3** was simple and straightforward as shown in Scheme 1. First, 4-(4′-methylbenzoyl)benzoic acid was esterified to yield **4** which was later brominated with NBS. The resulting bromomethyl ester of 4-(4′-bromomethylbenzoyl)benzoic acid, **5**, reacted with trimethylamine to produce a water-soluble ester **6**, which was then hydrolyzed to yield acid **7**. The exercise of esterification was to prevent the competition between the carboxylate group and trimethylamine.

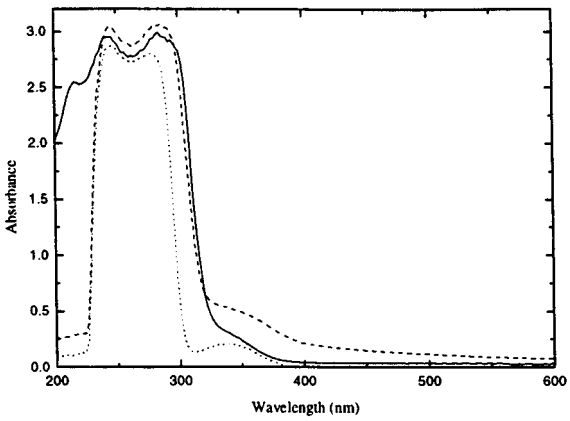

Figure 1. UV absorption spectra (···, benzophenone in CH_2Cl_2; —, compound **3** in H_2O; - - -, compound **3** in CH_2Cl_2).

Scheme 1

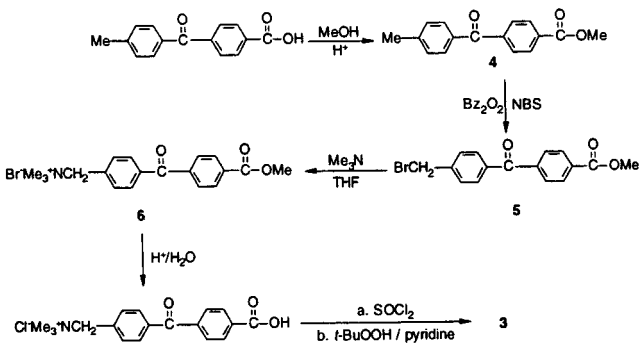

Compound **3** was characterized by its ^1H and ^{13}C NMR spectra. The presence of both carbonyl functional groups is evidenced by the two IR absorption bands, ν 1757 cm^{-1} (carbonyl of perester) and ν 1665 cm^{-1} (carbonyl of benzophenone). Perester **3** is soluble in both styrene (~0.1 g/mL) and water (0.1 g/mL or 10 wt %). Compared to perester **1** (water solubility > 1 g/mL), the introduction of a benzophenone unit reduces the water solubility noticeably. However, a 10% water solubility is more than adequate for polymerization applications. Surface activity of perester **3** was measured by its ability to change the surface tension of water. At 0.014 M, perester **3** lowered the surface tension of pure water (72 mN/m) to 45.6 mN/m. This value is comparable with that of SDS (36 mN/m, cmc = 0.0081 M)[40] and DTAB (37 mN/m, cmc = 0.0153 M)[41] at a comparable concentration. The UV absorption spectra of **3** in water and methylene chloride, respectively, and of benzophenone in methylene chloride are shown in Figure 1. The n → π^* transition of **3** is slightly blue shifted in water relative to that in methylene chloride due to solvent polarity change.[42] Comparing to **2** in methylene chloride, compound **3** has a similar molar absorptivity in water at 350 nm ($\epsilon_{350\ nm}$ = 226 L mol^{-1} cm^{-1}).

Perester **3** shows a strong oxidizing power when tested with potassium iodide. The rate constants for the formation of iodine are given in Table 1 for both peresters **3** and **1**. The pseudo-first-order rate constants indicate that perester **3** is a slightly stronger oxidizing agent than perester **1** in aqueous solution.[43] The

Table 1. Solubilities, Reaction Rate Constants with KI, and Decomposition Rate Constants (64 °C)

peroxide	solubility (g/mL)	k^a (min^{-1})	k^b (min^{-1})
3	0.1	0.003 58	0.002 52
1	>1	0.002 37	0.007 04

[a] [peroxide] = (5−10) × 10^{-5} M; [KI] = 5.5 × 10^{-2} M. [b] Thermal decomposition rate constant.

Scheme 2

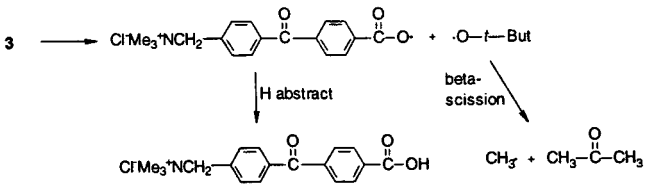

relative oxidation rates were also examined in the presence of surfactants. It was found that the oxidation rate for compound **3** with potassium iodide in the presence of DTAB (dodecyltrimethylammonium bromide) is 37 times higher than that in the absence of any surfactant. The oxidation rate for **3** with potassium iodide in the presence of SDS (dodecyl sulfate, sodium salt), however, is 35 times lower than that in an aqueous solution free from any surfactant. The results further indicate that compound **3** is strongly associated with the micelles formed by SDS or DTAB. The dioxy group is most likely located in the hydrophobic region of the micelles. In the presence of DTAB which concentration (0.02 M) is above its cmc (0.0153 M),[44] the positive charge of the surfactant increases the effective local concentration of iodide ions at the interface, so that the interaction between iodide and the dioxy group is enhanced. In the presence of SDS micelles ([C] = 0.01 M, cmc = 0.0081 M),[44] however, the local concentration of iodide at the interface is much lower because of the repulsion between the negatively charged iodide and SDS headgroups.

Decompositions of Perester 3 in Deuterium Oxide. The decomposition of compound **3** in deuterium oxide was monitored with ^{1}H NMR. In photoinduced decomposition, as the intensity of the *tert*-butyl peak of perester **3** decreased, a new peak at δ 2.19 increased. The δ 2.19 peak was assigned to the methyl group of acetone according to an authentic sample. An analysis of the reaction products indicates that the parent carboxylic acid **7** was the only product in addition to acetone. To account for the formation of these two products, a homolytic decomposition was proposed as the initial step (Scheme 2). The carboxylic acid **7** may be the result of a hydrogen abstraction by the carboxyl radical. A β-scission of the *tert*-butoxy radical may lead to the formation of an acetone and methyl radical. Although its fate is unclear at this point, the methyl radical is unlikely to yield any detectable product. One possible outlet for the radical could be methane via hydrogen abstraction. It was found that the quantum yields were greater than unity. With a higher initial peroxide concentration, the quantum yield became greater (Table 2). This is consistent with a chain decomposition mechanism involving the hydrogen abstraction by the carboxyl methyl radicals. In thermal decomposition, however, methanol was also found (>80% yield). To explain the formation of methanol, a heterolytic decomposition mechanism was proposed as the major decomposition pathway (Scheme 3).[45] The homolytic cleavage illustrated in Scheme 2 must be, if anything, a minor pathway for the decomposition of **3** under this condition.

Table 2. Photochemical Decomposition of Peroxides 3 and 2[2]

peroxide	[C] (M)	$k \times 10^4$ (s^{-1})	quantum yield
3[a]	0.0123	8.89	1.73[b]
3[a]	0.0271	6.70	3.36[c]
2[d]	0.0590	1.84	0.94[e]

[a] In deuterium oxide. [b] $I = 1.86 \times 10^{17}$ quanta/min. [c] $I = 1.32 \times 10^{17}$ quanta/min. [d] In benzene. [e] $I = 6.56 \times 10^{17}$ quanta/min.

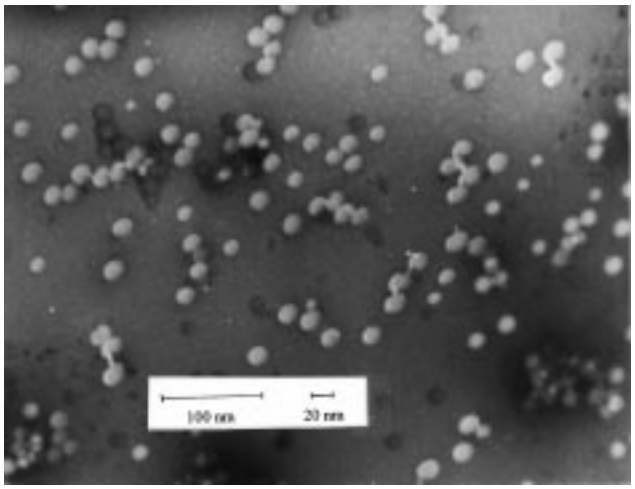

Figure 2. TEM photograph of a typical polymer latex produced by microemulsion polymerization of styrene with perester **3** as photoinitiator.

Scheme 3

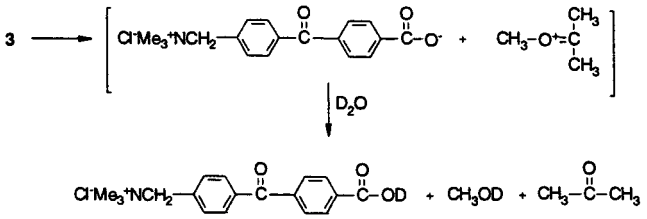

Structure of Microemulsions and Characterizations of Polystyrene Latices. All microemulsions prepared for this study were within one-phase regions according to their titrated partial phase diagrams.[27,46] They were optically transparent fluids and exhibited slightly higher viscosity than water. The monomer droplet size was estimated to be ca. 5 nm based on an aggregation number of 188 for DTAB in the presence of 4% styrene.[46]

The polymer latices obtained were spherical and relatively monodispersed (Figure 2). They were somewhat more translucent than the original microemulsions depending on their sizes and the amount of polystyrene. With a higher concentration of polystyrene or larger particle size, the latices appeared bluish. The polymer particles are generally larger (diameter ranging from 12.6 nm to 39.7 nm) than their parent monomer droplets (ca. 5 nm).

Photoinduced and Heat-Induced Polymerizations. Table 3 lists the results from the photoinduced and heat-induced polymerization of styrene in microemulsions prepared from a cationic (DTAB) or an anionic (SDS) surfactant. It is clear that the polymer particle size, molecular weight, and molecular weight distribution are directly influenced by the type of

Table 3. Photoinduced and Thermal-Induced Polymerization of Styrene in Microemulsion with DTAB and SDS[a]

microemulsion	polymerization time	conversion (%)	M_w ($\times 10^4$)	M_n ($\times 10^4$)	M_w/M_n	diameter (nm)
SDS, 14.91%	$h\nu = 20$ min	82.2	48.9	6.83	7.15	28.4
styrene, 3.98%	$\Delta = 7$ h	68.4	137.0	28.3	4.82	39.7
water, 81.11%						
DTAB, 14.40%	$h\nu = 20$ min	54.3	9.33	3.66	2.55	23.6
styrene, 4.00%	$\Delta = 7$ h	48.1	64.6	20.4	3.18	31.0
water, 81.60%						

[a] Perester concentration: 1.0 mM (based on water).

surfactant, mean of activation of the initiator, and the concentration of each component. For example, the polymer particles are significantly larger from the systems using an anionic surfactant than those from a cationic system. The polymers also have higher molecular weights and broader molecular weight distributions from SDS systems than those from DTAB systems. It is also clear from the results shown in Table 3 that, using either SDS or DTAB, heat-induced polymerization gave larger polymer particles and higher molecular weights than those generated photochemically.

In a microemulsion, the recombination of two radicals in a monomer droplet is expected to be fast due to the small sizes. To initiate the polymerization, the two radicals must separate. Microemulsion polymerization has a different nucleation mechanism compared with emulsion polymerization where monomer droplets simply provide a monomer reservoir due to low efficiency in capture of radicals. In microemulsion polymerization with KPS (potassium persulfate) or AIBN (azobisisobutyronitrile) as initiator, the nucleation is initiated with the entry of radicals into monomer droplets[22−24] because the sizes of the monomer droplets are small and surface areas are high so they can capture radicals efficiently. The conventional initiators such KPS, AIBN, and dibenzyl ketone are located in either the water or the oil phase in microemulsions. The decomposition of these initiators generate a small radical anion (from KPS) or radical (from AIBN and DBK). The nature of surfactant has almost no effect on the entry of radicals. However, the perester initiator in our study is amphiphilic. It is most likely located at the interface of the micelle. The KI study described above indicated that the perester is associated with the surfactant, regardless the type of surfactant (DTAB or SDS). When a charged initiator becomes incorporated in the monomer droplets, the interaction of the initiator and the surfactant has to be considered since the polymerization is initiated with the departure of one radical of the radical-pair from the interface to either the oil phase or water phase. Therefore, the surface-active perester is more sensitive to the type of surfactant. In the presence of anionic surfactant such as SDS, the cationic initiator is bound strongly with the negative surfactant on the monomer droplets. The departure of the one of the radicals is more difficult, and the recombination of radicals is efficient. This translates to fewer radicals available for the polymerization and leads to the production of a high molecular weight polymer. When a cationic surfactant such as DTAB is used, on other hand, the cationic radical leaves the monomer droplet more easily due to the repellence between the surfactant and the initiator. More radicals are available for polymerization in DTAB microemulsions, which again translates to a lower molecular weight, although it is believed that microemulsion is initiated within the monomer droplets. When a surface-active initiator which is predominately located at the interface of the micelles, the departure of one radical of the pair allows the counterpart radical to propagate. The exited radical could also enter another droplet and propagate. Nucleation in aqueous phase during the transfer of the exited radical to another monomer droplet is also possible.

Table 4. Polymerization of Styrene with Different Irradiation Times[a]

[initiator] (mM)	irrad time (min)	conversion (%)	M_w ($\times 10^4$)	M_n ($\times 10^4$)	M_w/M_n	diameter (nm)
1.0	10	34.8	9.01	3.87	2.33	23.7
	20	54.3	9.33	3.66	2.55	23.6
	30	58.3	9.63	4.36	2.21	25.0
	40	62.5	10.9	4.52	2.42	23.7
	60	67.8	11.1	4.85	2.29	24.3
	90	74.0	12.5	3.69	2.38	25.4
	150	86.6	33.1	5.39	6.14	29.4
2.0	10	38.7	6.48	3.14	2.07	18.4
	20	54.9	6.51	3.26	2.00	18.4
	30	59.4	6.93	3.39	2.05	18.7
	40	66.3	7.64	3.64	2.05	19.0
	60	71.8	7.51	2.97	2.53	19.0
	90	85.0	8.28	3.58	2.32	20.1
	150	89.2	8.80	3.72	2.36	20.3

[a] Styrene: 4% (by weight). DTAB/water = 15/85 (w/w).

The decomposition study described above also indicated that there are two decomposition pathways for the perester (Scheme 2). Although these two pathways are found in both heat-induced and photoinduced decomposition of the perester, the heterolytic cleavage is preferred in the heat-induced decomposition. Therefore, more homolytic cleavage is expected in the decomposition under irradiation and more radicals would be generated. A higher radical concentration translates to a lower average molecular weight of the polymers.

Evolution of Latex Particles. The profile of photoinduced polymerizations with DTAB as surfactant at different time intervals is shown in Table 4. Within 90 min, the molecular weight of polymers produced slightly increases. With 1.0 mM of initiator concentration, there is no significant change in molecular weight within 90 min of polymerization although monomer conversion increases with time. Because polymerization is believed to be initiated inside the small size of monomer droplet (formation of particles) and particles grow by recruiting other monomer droplets, recombination of two particles will be less likely. Particles grow with polymerization time, and higher molecular weights of polymer are obtained with longer time. However, further increasing polymerization will increase the chance that two particles recombine since much less monomer is available. This recombination may not apply to every particle and leads to broadening of the molecular weight distribution.

Effect of Surfactant Concentration. Particle size, molecular weight, and molecular weight distribution of polymers formed via photoinduced polymerizations with different DTAB concentrations are summarized in Table 5. It is clear that a higher surfactant concentration

Table 5. Polymerization of Styrene in Microemulsions with Different Surfactant Concentrations[a]

DTAB (g)	conversion (%)	N_p ($\times 10^{17}$)	M_w ($\times 10^4$)	M_n ($\times 10^4$)	M_w/M_n	diameter (nm)
0.5	72.1	8.19	10.6	5.07	2.09	17.9
1.0	45.7	7.49	7.35	3.10	2.37	16.0
1.5	20.0	5.29	4.55	2.20	2.07	15.1
1.8	10.7	4.90	2.63	1.46	1.80	13.7
2.0	4.80	2.98	1.94	1.12	1.73	12.6

[a] Styrene 0.2 g, water 8.16 g; initiator concentration 1.0 mM based on concentration; irradiation time 20 min.

Table 6. Polymerization of Styrene in Microemulsion with Different Initiator Concentrations

initiaton concentration (mM)	conversion (%)	M_w ($\times 10^4$)	M_n ($\times 10^4$)	M_w/M_n	diameter (nm)
2.5	55.7	5.80	2.70	2.15	15.5
2.0	54.9	6.51	3.26	2.00	18.8
1.5	55.2	7.59	3.82	2.33	19.9
1.0	54.3	9.66	3.66	2.55	23.6
0.5	15.2	12.2	3.95	3.09	25.5

[a] Styrene 4% (by weight); DTAB/water = 15/85 (w/w); irradiation time 20 min.

yields a lower conversion of monomers. Polymers produced with higher surfactant concentrations also have lower molecular weights and narrower molecular weight distributions. Increasing surfactant concentration increases the number of monomer droplets and decreases the amount of styrene in each droplet. The increase in the number of monomer droplets renders a decrease in the number of monomer droplets being polymerized (Table 5) and in the fraction of monomer droplets which can be polymerized at a given number of photons. As a consequence, the polymerization has a lower percent conversion. An increase in number of monomer droplets also decreases the size of monomer droplet (each monomer droplet contains less styrene) and leads to a lower molecular weight and smaller particles.

Effect of Initiator Concentration. Results in Table 6 show the particle size, molecular weight, and molecular weight distribution of polymers from photoinduced polymerizations in DTAB/styrene/water microemulsions with two different initiator concentrations. Polymers with lower molecular weight and small size are produced with higher initiator concentrations. log−log plots of molecular weight (M_w), particle diameter (D) of the polymer, and number of particles (N_p) against initiator concentration ([I]) show a linear relation between M_w, D, N_p and perester concentration (Figure 3). Dependencies of molecular weight (M_w), particle diameter (nm), and the number of particles on initiator concentration are −0.48, −0.30, and +1.64, respectively. The dependencies of molecular weight and particle size on initiator concentration are slightly greater than that of AIBN (−0.4 and −0.2, respectively) and KPS (−0.4 and −0.2, respectively) in a similar microemulsion system.[24] Since the dependency of latex features on initiator concentration are due to different efficiencies of the initiators in producing "effective radicals",[28] this indicates a stronger dependency of molecular weight on initiator concentration than that of AIBN and KPS. A higher initiator concentration translates to a higher flux of radicals; thus more monomer droplets become polymerized particles (N_p increases), and the probability for radicals to terminate the propagating polymer

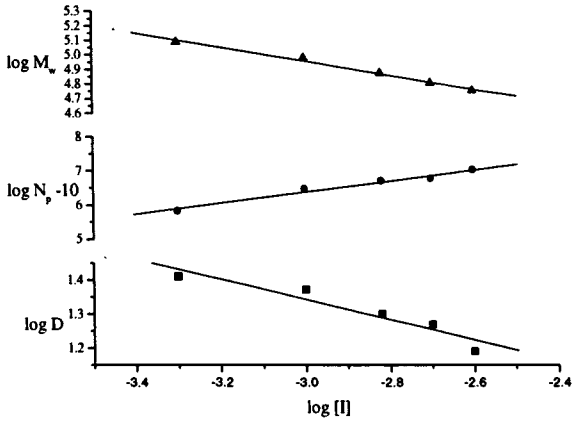

Figure 3. Dependency of molecular weight (M_w), number of particles (N_p), and particle diameter (D) on the initiator concentration.

Table 7. Polymerization of Styrene in Microemulsions with Different Styrene Concentrations[a]

styrene (w%)	conversion (%)	M_w ($\times 10^4$)	M_n ($\times 10^4$)	M_w/M_n	diameter (nm)
2	10.7	2.63	1.46	1.80	13.7
4	22.4	7.02	2.97	2.36	16.2
6	37.0	10.2	3.90	2.62	17.7
8	53.4	11.2	4.45	2.52	17.9

[a] DTAB/water = 15/85 (w/w); initiator concentration 1.0 mM (based on water); irradiation time 20 min.

becomes higher. As the result, the conversion is increased and the polymers obtained have lower molecular weights.

Effect of Styrene Concentration. The results in Table 7 show the particle size, molecular weight, and molecular weight distribution of polymers from photoinduced polymerizations with different styrene concentrations. The molecular weight of polystyrene and the percent conversion increase with the increase of monomer concentration. When the styrene concentration increases from 2% to 4%, the molecular weight distribution (MWD) is significantly broadened. However, MWD increases only slightly when styrene concentration increased from 4% to 8%. The study on the KI oxidation by perester **3** indicated that the perester is located at the interface of the microemulsion. The polymerization is predominantly initiated within monomer droplets with the departure of one of the two radicals generated at the interface, and particles grow by recruiting unpolymerized monomer droplets, so that molecular weight as well as particle size of polystyrene particles depends on the amount of styrene in each droplet (i.e., the size of monomer droplets). When other factors are kept unchanged, the particle size of polymers will depend on only the amount of styrene inside each droplets, i.e., the size of the monomer droplets. Polymers with higher molecular weight and larger particle size are expected from a higher concentration of styrene. Broader MWD at higher styrene concentration could be due to faster particle growth. When the styrene concentration is below 6% (by weight), the average molecular weight (M_w) is linearly related to the styrene concentration (Figure 4). The slope of such linear relationship is greater than unity. This is a strong indication that the increase in styrene concentration also changes the aggregation number of the surfactant molecules,[43] which results in a decrease in the number of monomer droplets. This effect levels off when the styrene con-

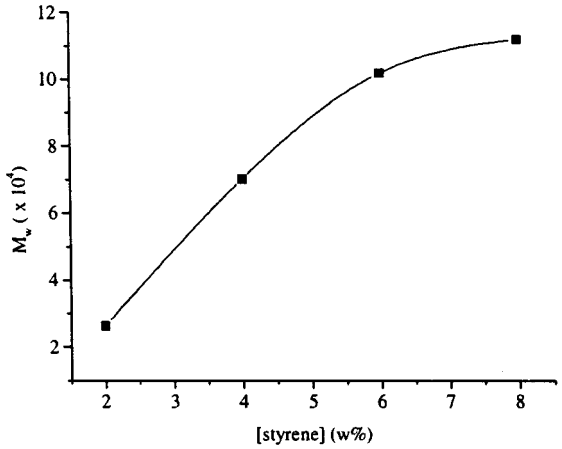

Figure 4. Dependency of molecular weight (M_w) on styrene concentration.

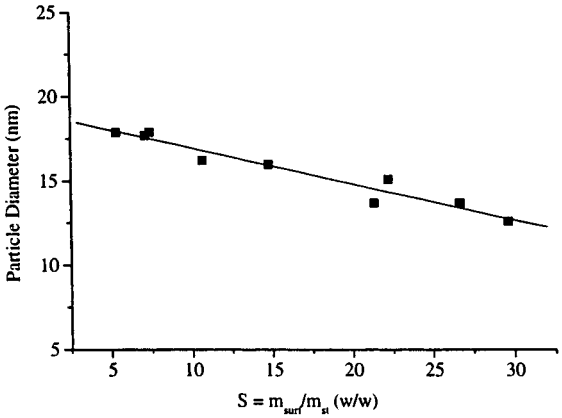

Figure 5. Dependency of particle diameter on the surfactant (m_{surf}) to monomer (m_{st}) ratio (S).

centration is higher than 6%. It is recognized that the particle size of polystyrene latices produced from microemulsion polymerization can be linearly correlated to the amount of surfactactant.[25] This linear relationship is also found in our present work (Figure 5), an indication that the model described in Antonietti's work is also applicable to a system with a surface-active initiator.

Conclusion

When a surface-active perester is used as a photoinitiator in microemulsion polymerizations, polymers with high molecular weights and narrow molecular weight distributions are obtained. The molecular weight, molecular weight distribution, and particle size can be controlled by the type of the surfactant, concentration of the initiator, monomer, surfactant, and the means by which the initiator is activated. A polymerization mechanism was proposed for microemulsion polymerization of styrene with a surface-active photoinitiator: polymerization is initiated within the monomer droplets with the departure of one of the radical pair which were generated at the interface. The possibilities of homogeneous nucleation and nucleation by entry of the exited radical into another monomer droplet were not excluded. A detailed analysis on the behavior of a charged radical initiator in a microemulsion before and during polymerization may provide a useful tool to investigate the polymerization mechanism in terms of the interaction between the initiator and the surfactant interface. The information may also lead to a better design for a peroxide initiator that can initiate the polymerization with the desired kinetics and produce polymer particles with desired characteristics such as a lower level of monomer residue.

References and Notes

(1) Candau, F. In *Encyclopedia of polymer science and engineering*, 2nd ed.; Mark, H. F., Birkales, N. M., Overberger, C. G., Menges, G., Eds.; John Wiley & Sons: New York, 1987; pp 718−724.
(2) Thijs, L.; Gupta, S. N.; Neckers, D. C. *J. Org. Chem.* **1979**, *44*, 4123.
(3) Mikhael, M. G.; Padias, A. B.; Hall, H. K., Jr. *Macromolecules* **1995**, *28*, 5951.
(4) Kutal, C. R. PCT Internat. Appl. WO 93 10,483, 1993.
(5) He, J.-H.; Mendoza, V. S. *J. Polym. Sci., Polym. Chem. Ed.* **1996**, *34*, 2809.
(6) Allen, N. S.; Catalina, F.; Green, P. N.; Green, W. A. *Eur. Polym. J.* **1986**, *22*, 347.
(7) Fouassier, J. P.; Lougnot, D. J. *J. Appl. Polymer Sci.* **1986**, *32*, 6209.
(8) Lougnot, D. J.; Fouassier, J. P. *J. Polym. Sci., Polym. Chem. Ed.* **1988**, *26*, 1021.
(9) Majima, T.; Weber, W.; Schnabel, W. *Makromol. Chem.* **1991**, *192*, 2307.
(10) Ivanchev, S. S.; Pavljuchenko, V. N.; Byrdina, N. A. *J. Polym. Sci., Polym. Chem. Ed.* **1987**, *25*, 47.
(11) Ando, W., Ed. *Organic Peroxides*; John Wiley & Sons: New York, 1992.
(12) Lu, M. Y.; Bao, R.; Liu, W.; Li, Y. *J. Org. Chem.* **1995**, *60*, 5341.
(13) Hoar, J. P.; Schulman, J. H. *Nature* **1943**, *152*, 102.
(14) Tadros, Th. F. *Adv. Colloid Interface Sci.* **1993**, *46*, 1−47.
(15) Candau, F. In *Polymerization in organized media*; Paleos, C. M., Ed.; Gordon and Breach Science Publishers: Philadelphia, PA, 1992; pp 215−282.
(16) Antonietti, M.; Basten, R.; Lohmann, S. *Macromol. Chem. Phys.* **1995**, *196*, 441−466.
(17) Stoffer, J. O.; Bone, T. *J. Dispersion Sci. Technol.* **1980**, *1*, 37.
(18) Stoffer, J. O.; Bone, T. *J. Polym. Sci., Polym. Chem. Ed.* **1980**, *18*, 2641.
(19) Atik; S. S.; Thomas, J. K. *J. Am. Chem. Soc.* **1981**, *103*, 4279.
(20) Candau, F.; Leong, Y. S.; Pouyet, G.; Candau, S. J. *J. Colloid Interface Sci.* **1984**, *101*, 167.
(21) Candau, F.; Leong, Y. S.; Fitch, R. M. *J. Polym. Sci., Polym. Chem. Ed.* **1985**, *23*, 193.
(22) Guo, J. S.; El-Aasser, M. S.; Vanderhoff, J. W. *J. Polym. Sci., Polym. Chem. Ed.* **1989**, *27*, 691−710.
(23) Gan, L. M.; Chew, C. H.; Lye, I. *Makromol. Chem.* **1992**, *193*, 1249−1260.
(24) Puig, J. E.; Perez-Luna, V. H.; Perez-Gonzalez, M.; Macias, E. R.; Rodriguez, B. E.; Kaler, E. W. *Colloid Polym. Sci.* **1993**, *271*, 114−123.
(25) Antonietti, M.; Bremser, W.; Muschenborn, D.; Rosenauer, C.; Schupp, B. *Macromolecules* **1991**, *24*, 6636−6643.
(26) Jayakrishnan, A.; Shaw, D. O. *J. Polym. Sci., Polym. Lett.* **1984**, *22*, 31.
(27) Perez-Luna, V. H.; Puig, J. E.; Castano, V. M.; Rodriguez, B. E.; Murthy, A. K.; Kaler, E. W. *Langmuir* **1990**, *6*, 1040−1044.
(28) Gan, L. M.; Chew, C. H.; Lim, J. H.; Lee, K. C.; Gan, L. H. *Colloid Polym. Sci.* **1994**, *272*, 1082−1089.
(29) Gan, L. M.; Chew, C. H.; Lee, K. C. *Polymer* **1994**, *35*, 2659−2664.
(30) Kuo, P.-L.; Turro, N. J.; Tseng, C.-M.; El-Aasser, S.; Vanderhoff, J. W. *Macromolecules* **1987**, *20*, 1216−1221.
(31) Gupta, S. N.; Thijs, L.; Neckers, D. C. *J. Polym. Sci., Polym. Chem. Ed.* **1981**, *19*, 855. Smith, M. E. *J. Am. Chem. Soc.* **1921**, *43*, 1920.
(32) Chu, B. *Laser Light Scattering*; Academic Press: New York, 1974.
(33) Pecora, R. *Dynamic Light Scattering*; Plenum Press: New York, 1976.
(34) Tokumaru, K. *Res. Chem. Intermed.* **1996**, *22*, 255.
(35) Monroe, B. M.; Weed, G. C. *Chem. Rev.* **1993**, *93*, 435.
(36) Neckers, D. C. U.S. Patent 4,416,826, 1983; *Chem. Abstr.* **1984**, *100*, 86286r.

(37) Neckers, D. C. U.S. Patent 4,752,649, 1988; *Chem. Abstr.* **1988**, *109*, 211626r.
(38) Allen, N. S.; Hardy, S. J.; Jacobine, A. F.; Glaser, D. M.; Catalina, F. *Eur. Polym. J.* **1989**, *25*, 1219.
(39) Allen, N. S.; Hardy, S. J.; Jacobine, A. F.; Glaser, D. M.; Catalina, F.; Navaratnam, S.; Parsons, B. J. In *Radiation Curing of Polymers II*; Randell, D. R., Ed.; The Royal Society of Chemistry: Cambridge, England, 1991.
(40) Breuer, M. M.; Robb, I. D. *Chem. Ind.* **1972**, *13*, 530−535.
(41) McGrath, K. M. *Langmuir* **1995**, *11*, 1835−1839.
(42) Skoog, A. D. *Principles of Instrument Analysis*; Saunders College Publishing: New York, 1985.
(43) Blomquist, A. T.; Berstein, I. A. *J. Am. Chem. Soc.* **1951**, *73*, 5546.
(44) Hiemenz, P. C. *Principles of Colloid and Surface Chemistry*; Marcel Dekker: New York, 1986; p 432.
(45) Wistuba, E.; Ruchardt, C. *Tetrahedron Lett.* **1981**, *22*, 3389.
(46) Full, A. P.; Kaler, E. W.; Arellano, J.; Puig, J. E. *Macromolecules* **1996**, *29*, 2764−2775.

MA970907Q